arXiv:cond-mat/9910291v1 [cond-mat.str-el] 19 Oct 1999

Reconciling the correlation length for high-spin Heisenberg antiferromagnets

B.B. Beard[a], V. Chudnovsky[b], and P. Keller-Marxer[c]
[a] Departments of Physics and Mechanical Engineering, Christian Brothers University, Memphis, TN 38104
[b] Department of Physics, Massachusetts Institute of Technology, Cambridge, MA 02139
[c] Institut für Theoretische Physik, Universität Bern, CH-3012 Bern, Switzerland

(February 1, 2008)

We present numerical results for the antiferromagnetic Heisenberg model (AFHM) that definitively confirm that chiral perturbation theory, corrected for cutoff effects in the AFHM, leads to a correct field-theoretical description of the low-temperature behavior of the spin correlation length for spins $S \geq 1/2$. With two independent quantum Monte Carlo algorithms and a finite-size-scaling technique, we explore correlation lengths up to $\xi \approx 10^5$ lattice spacings a for spins $S = 1$ and $5/2$. We show how the recent prediction of cutoff effects by P. Hasenfratz is approached for moderate $\xi/a = \mathcal{O}(100)$, and smoothly connects with other approaches to modeling the AFHM at smaller correlation lengths.

75.10.Jm,02.70.Lq,31.15.Kb,71.10.Fd

In the past decade there has been a resurgence of interest in the quantum Heisenberg model. This interest is mainly due to the discovery that the undoped, insulating precursors of lamellar high-T_c superconducting copper oxides are well-described by the spin $S = 1/2$ two-dimensional (2-d) antiferromagnetic Heisenberg model (AFHM) on a square lattice. The field theories that describe this model at low temperatures share the property of asymptotic freedom with the theories that describe elementary particles, thus earning a share of attention from the high-energy physics community as well.

The low-temperature physics of the AFHM is dominated by magnons. The magnon interactions are described by the 2-d classical continuum $O(3)$ non-linear σ-model at large correlation lengths. This is an extensively studied model in field theory, offering various known exact results that can be exploited for the prediction of the correlation length $\xi(T)$ in the Heisenberg model at low temperatures. The challenge is to find a proper way to connect the parameters of the quantum Heisenberg model with the coupling of the σ-model. Several approaches to this problem exist. Chakravarty, Halperin, and Nelson [1] used renormalization group arguments to predict the leading behavior of $\xi(T)$. Hasenfratz and Niedermayer [2,3] utilized analytical results for the σ-model to refine the prediction, and they used chiral perturbation theory (CPT) [4] for the AFHM [5] to connect the parameters of the two models.

Neutron scattering experiments on $S = 1/2$ antiferromagnets such as $Sr_2CuO_2Cl_2$ generally agree with this prediction [6]. However, higher-spin antiferromagnets have remained problematic. Widely different techniques – including experiment [7–9], high-temperature series expansion [10], quantum Monte Carlo simulation for $S = 1$ [11], and semi-classical approximation [12] – all showed large deviations from the field-theoretical prediction by as much as 75% for $\xi < 200$ lattice spacings, which is the regime accessible in experiments on La_2NiO_4 ($S = 1$) and Rb_2MnF_4 ($S = 5/2$). These results suggest that a serious discrepancy would persist to really large, macroscopic correlation lengths for $S > 1/2$, which is highly unsatisfactory on theoretical grounds.

In a recent paper [13], Hasenfratz argues that this discrepancy is due to cutoff effects in the AFHM, which increase strongly with spin S. When large, they can not be described anymore with the effective approach of CPT. Hasenfratz used spin-wave expansion to calculate the cutoff effects, and he showed the proper way to incorporate them into the CPT result.

In this Letter we show via extensive quantum Monte Carlo (QMC) calculations that this correction indeed accounts for the severe spin dependence of the correlation length. Our data connect the regime of large and moderate correlation lengths, where "CPT+cutoff" applies, with the regime of small correlation lengths where high-temperature and semi-classical results apply. The diverse approaches are thereby reconciled. We also provide evidence that by $S = 5/2$ the residual deviation at small correlation lengths, possibly due to the missing higher-order terms in the analytical calculations, has essentially reached the classical $S \to \infty$ limit.

Consider the 2-d quantum Heisenberg model with nearest-neighbor interaction on an $L \times L$ lattice with lattice spacing a and periodic boundary conditions,

$$H = J \sum_{x,\mu} \vec{S}_x \cdot \vec{S}_{x+\hat{\mu}} \ , \quad \vec{S}_x^{\,2} = S(S+1) \ , \tag{1}$$

where $J > 0$ is the antiferromagnetic exchange coupling, $\hat{\mu}$ denotes the two primitive translation vectors of the unit cell, and $\vec{S}_x$ is the spin operator at position x.

The $O(3)$ symmetry of this Hamilton operator is spontaneously broken at zero temperature, and the model exhibits long-range antiferromagnetic order in the ground state. As a consequence, the model has two massless, relativistic Goldstone bosons (called magnons or spin waves). However, the Mermin-Wagner-Coleman theorem [14] rules out Goldstone bosons in two dimensions at nonzero temperature. Instead, the AFHM magnons acquire a mass $c/\xi(T)$ where c is the spin-wave velocity. (We set $\hbar$ and k_B to unity.) In fact, the σ-model is known to have a non-perturbatively generated mass gap, and the leading exponential behavior of the correlation length in the AFHM is a consequence of asymptotic freedom in the σ-model.

The partition function of the 2-d quantum spin model in Eq. (1) can be represented by a path integral [15] of a classical model with an additional ("time") dimension. The continuous coordinate x_3 of this periodic Euclidean-time dimension has extent c/T. When $T \to 0$, the correlation length grows exponentially, and becomes much larger than the length scale c/T. The system then appears dimensionally reduced to a thin slab with two infinite space directions and an extent $c/T \ll \xi(T)$ in the Euclidean-time direction. This is just a special regularization of the σ-model.

Hasenfratz and Niedermayer [2] used CPT for the AFHM [5], as well as the exact mass gap [3] and the 3-loop β-function [16] of the σ-model to derive the asymptotic prediction for the spin correlation length in the AFHM:

$$\xi_{\mathrm{CH_2N_2}} = \frac{e}{8}\frac{c}{2\pi\rho_s}\exp\left(\frac{2\pi\rho_s}{T}\right)\left[1-\frac{T}{4\pi\rho_s}+\mathcal{O}\left(T^2\right)\right]. \tag{2}$$

The values of spin stiffness ρ_s and spin-wave velocity c are not fixed by CPT, but they can be estimated by, for example, spin-wave expansion (SWE) [17] or fits from QMC data [18,19]. Calculating the $\mathcal{O}(T^2)$ corrections in CPT introduces new, unknown parameters. We call Eq. (2) the $\mathrm{CH_2N_2}$ formula after its parents Chakravarty, Halperin, Nelson, Hasenfratz, and Niedermayer.

The QMC data presented in this Letter confirm that the discrepancy between $\mathrm{CH_2N_2}$ and the $S > 1/2$ AFHM correlation length indeed is severe, and it persists to macroscopic correlation lengths $\xi/a \gg 10^5$. This situation is unsatisfactory since a mapping of the AFHM onto the σ-model must be valid for smaller correlation lengths, too, due to the dimensional reduction described above. In particular, this mapping is valid *beyond* the regime of "renormalized classical scaling" [20] near $T = 0$ (where Eq. (2) unquestionably is valid for any S). The virulent discrepancy indicates a shortcoming in the technique that connects the coupling of the σ-model with the AFHM parameters ρ_s and T using CPT for large spin.

In his recent calculation [13], Hasenfratz used bilinear spin-wave expansion to modify this connection, taking into account cutoff effects in the AFHM. In the present study, we also account for a minor refinement of the result by Hasenfratz: a part of the quadratic temperature dependence, coming from known terms in the spin-wave expansion of the coupling of the σ-model, is incorporated. The resulting $\mathrm{CH_3N_2B}$ formula is (with $t \equiv T/(2\pi\rho_s)$)

$$\begin{aligned}\xi_{\mathrm{CH_3N_2B}} &= \frac{e}{8}\frac{c}{2\pi\rho_s}\exp\left(\frac{1}{t}\right)\exp\left(-C(\gamma)\right)\\ &\quad\times\left[1-\frac{1}{2}t+\frac{27}{32}t^2+\mathcal{O}\left(T^2\right)\right].\end{aligned} \tag{3}$$

The parameter $\gamma \equiv 2JS/T$ brings in the explicit spin dependence. In Ref. [13], $\exp(-C(\gamma))$ is expressed as an integral of familiar spin-wave quantities over the first Brillouin zone. The asymptotic $T \to 0$ (S fixed) behavior is $C(\gamma \to \infty) \sim \gamma^{-2}$, so the $\mathrm{CH_2N_2}$ formula, Eq. (2), is recovered in this limit. The effect of the aforementioned refinement is simply to add the term $(27/32)t^2$ to the polynomial. (This term is only a part of the $\mathcal{O}(T^2)$ correction.)

In Ref. [21], an efficient continuous Euclidean-time QMC algorithm [18,19,22] was used to study the $S = 1/2$ AFHM correlation length up to 350,000 lattice spacings. For this purpose, a finite-size-scaling technique, developed by Caracciolo *et al.* ("CEFPS") [23] for the σ-model, was applied to the AFHM finite-volume $\xi(L)$ data. That study confirmed the validity of the "no cutoff effects" $\mathrm{CH_2N_2}$ formula, Eq. (2), but only for large $\xi/a \approx 10^5$. By fitting a naïve quadratic term αt^2 in the polynomial factor of $\mathrm{CH_2N_2}$, good agreement was achieved down to $\xi/a \approx 100$ (yielding $\alpha = -0.75(5)$).

For $S > 1/2$ we used two independent QMC algorithms. One is a higher-spin generalization of the $S = 1/2$ continuous-Euclidean-time loop-cluster algorithm first described in Ref. [19]. The other one is a "traditional" discrete-Euclidean-time loop-cluster algorithm for arbitrary S, based on a method proposed by Kawashima and Gubernatis [24]. Results from these two codes were cross-checked and agree for all spins within statistical errors, which gives a high degree of confidence to our calculations.

The finite-volume correlation lengths $\xi(L)$ were calculated using a second-moment method, similar to Eq. (4.13) in Ref. [25]. Afterwards, the CEFPS finite-size-scaling method was applied. This method expresses $\xi(2L)/\xi(L)$ as a universal function $F(\xi(L)/L)$ – applicable to all models within the universality class of the 2-d lattice-regularized nearest-neighbour $O(3)$ non-linear σ-model. Iteration of $F(\xi(L)/L)$ yields $\xi \equiv \xi(L \to \infty)$. Unlike the case for $S = 1/2$, we found that for $S > 1/2$ and our level of precision ($\approx 0.2\%$ for $\xi(L)$), it is not necessary to incorporate any correction for scaling violations, even for lattice sizes as small as $L/a \approx 10$. The maximum ξ/a generated in our study are approximately 170,000 for $S = 1$ and 135,000 for $S = 5/2$ [27]. Note that it is the finite-size scaling technique that enables the estimation of correlation lengths much larger than direct measurement allows (cf. Ref. [11], which achieved a maximum $\xi/a = 24.94(7)$ at $t = 0.18$ on a square lattice with side length $L/a = 200$). Details of our algorithms, improved estimators, finite-size-scaling technique, and calculation of $\xi(L)$ will be provided in a separate paper [26].

Figure 1 shows the QMC data plotted on a Memphis chart, where we divide ξ by the leading (2-loop) term $(e/8)(c/2\pi\rho_s)\exp(1/t)$ and plot versus t. For $S = 1/2$, the agreement between QMC and CH_3N_2B down to $\xi/a \approx 10$ ($t \approx 0.3$) is striking. For $S > 1/2$ we find that the QMC data smoothly merge into the CH_3N_2B predictions at $\xi/a > 100$ ($t < 0.15$) for $S = 1$, and $\xi/a > 500$ ($t < 0.10$) for $S = 5/2$. The agreement in each case degrades above some temperature. This is to be expected because CH_3N_2B leaves out higher-order terms from the CPT and spin-wave expansions. In addition, at high temperatures the field-theoretical requirements $\xi \gg c/T$ and $\xi \gg a$ are no longer satisfied, and predictions such as CH_3N_2B become meaningless. In our figures we plot the CH_3N_2B predictions only for $\xi/a \geq 3$.

Ref. [21] found that for $S = 1/2$, the true value of spin stiffness ρ_s is about 3% higher than the value predicted by third-order spin-wave theory (SW3). We find that comparison of QMC data with CH_3N_2B for $S = 1/2$ is in agreement with the fitted values of $\rho_s = 0.1800(5)$ and $c = 1.657(2)$ found in Ref. [21] (we set J and a to unity). That study combined the correlation length data fit to CH_2N_2, Eq. (2), with a fit of finite-volume magnetic susceptibilities [18,19] to the predictions of CPT for the finite-size and temperature effects in the AFHM [5]. High fit precision was achieved by exploiting this combination. We will present a similar study for the full range of spins $S \leq 5/2$ in a separate paper [26].

For this Letter, we have choosen a different approach which only involves the correlation length. We demonstrate that for $S > 1$ one can directly rely on the SW3 results [17] to achieve a consistent connection between the QMC data and CH_3N_2B. For the $S = 1$ case we find that the SW3 predictions $\rho_s^{\mathrm{sw3}} = 0.869$ and $c^{\mathrm{sw3}} = 3.067$ are nearly correct. Our two-parameter fit gives $\rho_s/\rho_s^{\mathrm{sw3}} = 1.005(3)$ and $c/c^{\mathrm{sw3}} = 0.98(2)$. These ratios correspond to $\rho_s = 0.8733(23)$ and $c = 3.01(6)$. The fit includes the $\xi/a > 100$ ($t < 0.15$) data in Figure 1, and has $\chi^2/\mathrm{d.o.f.} = 1.085$ with 58 degrees of freedom (which corresponds to a significance level $p = 30.5\%$). These values of ρ_s and c are used in the figures for $S = 1$.

Although the relative deviations from SW3 (0.5(3)% for ρ_s and $-2(2)\%$ for c) seem small, there is in fact a serious discrepancy. Using the SW3 values $(\rho_s^{\mathrm{sw3}}, c^{\mathrm{sw3}})$ in CH_3N_2B and comparing to the QMC ξ gives $\chi^2/60 = 1.39$ (a poor fit, with $p = 2.5\%$). Compared to the two-parameter fit, SW3 has $\Delta\chi^2 = +20.2$ (i.e., outside the 99.99% confidence region). The reason the near-overlap with SW3 is deceptive is that the fit parameters ρ_s and c are strongly anticorrelated (with correlation coefficient $r = -0.977$). Interestingly, the major axis of the nearly degenerate error ellipse is almost orthogonal to the curves of constant $\theta \equiv \rho_s/c^2$. In particular, the 68.3% confidence region for the joint probability distribution of ρ_s and c (enclosed by the $\Delta\chi^2 = +2.30$ ellipse) intersects the curve $\rho_s/c^2 = \theta^{\mathrm{sw3}}$. In other words, this 68.3% confidence region contains (ρ_s, c) values which are consistent with $\theta = \theta^{\mathrm{sw3}}$. We are thus motivated to check how close to ρ_s^{sw3} and c^{sw3} the corresponding single-parameter-fit values could in fact be.

To do this, we set $\theta_{S=1} = \theta_{S=1}^{\mathrm{sw3}} = 0.09238$ and performed a fit with the same set of $S = 1$ QMC data, with (ρ_s, c) constrained to the one-dimensional parameter subspace $\rho_s = \theta^{\mathrm{sw3}} c^2$. As an upper bound for the error associated with the assumption $\theta_{S=1} = \theta_{S=1}^{\mathrm{sw3}}$, we took from Ref. [21] the 4.4% deviation between $\theta_{S=1/2}^{\mathrm{sw3}} = 0.06277$ and that study's result $\theta_{S=1/2} = 0.06556$. This choice is conservative since SWE is an expansion in powers of $1/S$, and is expected to become more accurate as spin increases. Upon refitting, we found $\rho_s/\rho_s^{\mathrm{sw3}} = 1.0024(27)$, $c/c^{\mathrm{sw3}} = 1.001(21)$, and $\chi^2/59 = 1.083$ ($p = 30.8\%$). These ratios correspond to $\rho_s = 0.8711(24)$ and $c = 3.07(6)$. (The difference between the one- and two-parameter fits would not be visible in Figure 1.) Note the errors here are dominated by the conservative 4.4% uncertainty in $\theta_{S=1}$; the actual errors are bound to be smaller.

For $S = 5/2$, we could not identify any deviation from the SW3 values $\rho_s^{\mathrm{sw3}} = 5.9444$ and $c^{\mathrm{sw3}} = 7.3005$. We found $\chi^2/14 = 1.194$ ($p = 27.2\%$) for the data with $\xi/a > 500$. These SW3 values of ρ_s and c are used in the figures for $S = 5/2$.

Figure 2 shows the situation for $S = 5/2$ in more detail. There is an intermediate regime between $\xi/a \approx 500$ ($t \approx 0.10$), where CH_3N_2B starts to deviate, and $\xi/a \approx 12$ ($t \approx 0.15$), where the high-temperature-series expansion (HTE) [10] starts to fail. Most of the experimental data on Rb_2MnF_4 [9] fall into this "gap", which exists similarly for $S = 1$. At least for large spin $S = 5/2$, this intermediate regime is correctly described by the semi-classical approximation known as the pure-quantum self-consistent harmonic approximation (PQSCHA) [12]. The diverse approaches collectively describe the $S = 5/2$ correlation length from extremely small to extremely large values.

We note that a residual discrepancy between CH_3N_2B and numerical data persists in the classical limit $S \to \infty$, where the AFHM becomes the 2-d lattice-regularized nearest-neighbour $O(3)$ non-linear σ-model. Predictions for this model are available from analytical calculations [28] ($\xi/a \geq 10^5$), Monte Carlo simulation [23,29] ($10 \leq \xi/a \leq 10^5$), and series expansion [10]($\xi/a \leq 10$). Hasenfratz [13] also supplies the $\gamma \to 0$ form for the correction $\exp(-C(\gamma))$, which enables the computation of the classical $S \to \infty$ limit of Eq. (3). In Figure 3, we plot the ratio of ξ to the CH_3N_2B prediction for $S = 1/2, 1, 5/2$, and ∞ versus $1/\log_{10}(\xi)$. By $S = 5/2$ the discrepancy between the numerical data and CH_3N_2B has essentially reached the classical $S \to \infty$ limit. This means that the reasons for the residual discrepancy, including finite-order effects of the CPT and spin-wave expansions, are the same for the quantum AFHM and the classical σ-model.

In conclusion, the cutoff correction accounts for the overall spin dependence of the correlation length. The spin stiffness and spin-wave velocity approach the spin-wave theory predictions rapidly. The diverse approaches to the AFHM for higher-spin are complementary.

We thank U.-J. Wiese, P. Hasenfratz, F. Niedermayer, and P. Verrucchi for enlightening discussions. We also thank P. Verrucchi, R. Singh, N. Elstner, R.L. Leheny, and R.J. Christianson for use of their data. The work of VC was supported in part by the DOE under cooperative research agreement #DF-FC02-94ER40818. The work of PKM was supported in part by Schweizerischer Nationalfonds.

---

[1] S. Chakravarty, B.I. Halperin, and D.R. Nelson, Phys. Rev. B **39**, 2344 (1989).
[2] P. Hasenfratz and F. Niedermayer, Phys. Lett. B **268**, 231 (1991).
[3] P. Hasenfratz, M. Maggiore, and F. Niedermayer, Phys. Lett. B **245**, 522 (1990); P. Hasenfratz and F. Niedermayer, Phys. Lett. B **245**, 529 (1990).
[4] J. Gasser and H. Leutwyler, Ann. of Phys. **158**, 142 (1984).
[5] P. Hasenfratz and H. Leutwyler, Nucl. Phys. B **343**, 241 (1990); P. Hasenfratz and F. Niedermayer, Z. Phys. B **92**, 91 (1993).
[6] M. Greven *et al.*, Phys. Rev. Lett. **72**, 1096 (1994); Z. Phys. B **96**, 465 (1995).
[7] K. Nakajima *et al.*, Z. Phys. B **96**, 479 (1995).
[8] Y. S. Lee *et al.*, Eur. Phys. J. B **5**, 15 (1998).
[9] R.L. Leheny, R.J. Christianson, R.J. Birgeneau, and R.W. Erwin, Phys. Rev. Lett. **82**, 418 (1999).
[10] N. Elstner *et al.*, Phys. Rev. Lett. **75**, 938 (1995).
[11] K. Harada, M. Troyer, and N. Kawashima, J. Phys. Soc. Jpn. **67**, 1130 (1998).
[12] A. Cuccoli, V. Tognetti, P. Verrucchi, and R. Vaia, Phys. Rev. B **58**, 14151 (1998).
[13] P. Hasenfratz, cond-mat/9901355, to appear in Eur. Phys. J. B.
[14] N.D. Mermin and H. Wagner, Phys. Rev. Lett. **17**, 1133 (1966); S. Coleman, Commun. Math. Phys. **31**, 259 (1973).
[15] See, for example, J.R. Klauder and B.-S. Skagerstam: *Coherent States*, World Scientific, 1985.
[16] E. Brézin and S. Hikami, J. Phys. A **11**, 1141 (1978).
[17] J. Igarashi, Phys. Rev. B **46**, 10763 (1992); Z. Weihong, J. Oitmaa, and C.J. Hamer, Phys. Rev. B **43**, 8321 (1991); C. Hamer, Z. Weihong, and J. Oitmaa, Phys. Rev. B **50**, 6877 (1994).
[18] U.-J. Wiese and H.-P. Ying, Z. Phys. B **93**, 147 (1994).
[19] B.B. Beard and U.-J. Wiese, Phys. Rev. Lett. **77**, 5130 (1996).
[20] S. Chakravarty, B.I. Halperin, and D.R. Nelson, Phys. Rev. Lett. **60**, 1057 (1988); A. Sokol, N. Elstner, and R.R.P. Singh, cond-mat/9505148.
[21] B.B. Beard, R.J. Birgeneau, M. Greven, and U.-J. Wiese, Phys. Rev. Lett. **80**, 1742 (1998).
[22] H.G. Evertz, G. Lana, and M. Marcu, Phys. Rev. Lett. **70**, 875 (1993).
[23] S. Caracciolo *et al.*, Phys. Rev. Lett. **75**, 1891 (1995).
[24] N. Kawashima and J.E. Gubernatis, Phys. Rev. Lett. **73**, 1295 (1994); J. Stat. Phys. **80**, 169 (1995).
[25] S. Caracciolo *et al.*, Nucl. Phys. B **403**, 475 (1993).
[26] B.B. Beard, V. Chudnovsky, and P. Keller-Marxer, in preparation.
[27] The full set of correlation length data is available at http://www.cbu.edu/~bbbeard/highspin.htm.
[28] B. Allés, G. Cella, M. Dilaver, and Y. Gündüç, Phys. Rev. D **59**, 067703 (1999); D.-S. Shin, Nucl. Phys. B **546**, 669 (1999).
[29] J.-K. Kim, Phys. Rev. D **50**, 4663 (1994).

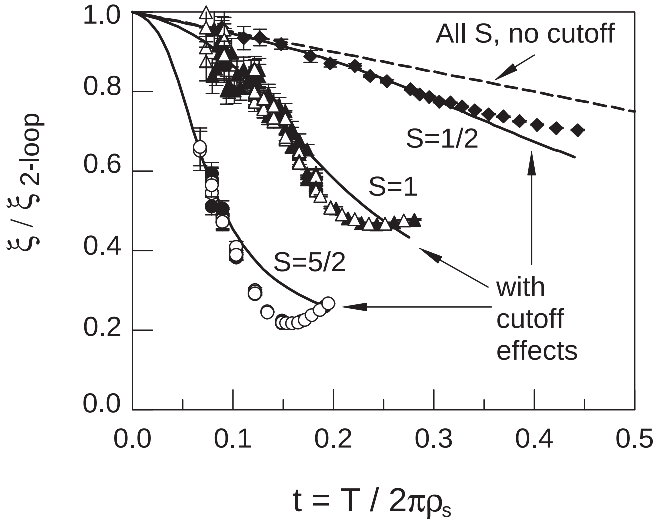

FIG. 1. Memphis chart for the AFHM. Correlation length QMC data and theoretical predictions are normalized by the leading (2-loop) prediction $(e/8)(c/2\pi\rho_s)\exp(1/t)$. Solid lines are the CH_3N_2B predictions, Eq. (3). Dashed line is the spin-independent "no cutoff effects" prediction CH_2N_2, Eq. (2). QMC data for $S = 1/2$ (diamonds), $S = 1$ (triangles), and $S = 5/2$ (circles); solid (open) symbols are from the continuous (discrete) Euclidean-time algorithm. The QMC data smoothly merge into CH_3N_2B at low temperatures.

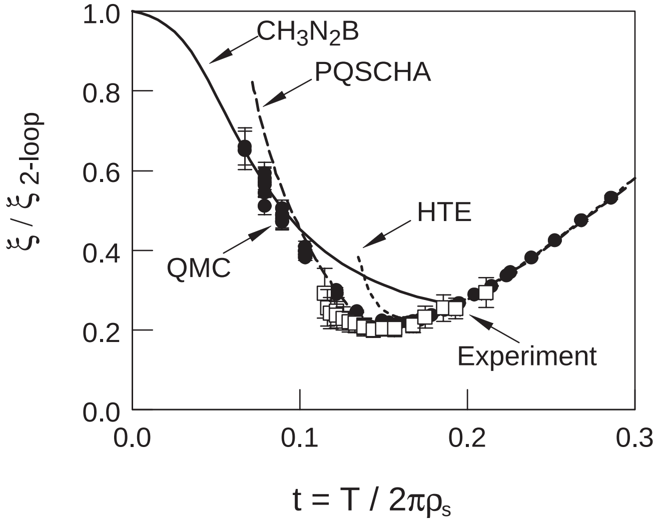

FIG. 2. Memphis chart for $S = 5/2$, showing CH_3N_2B (solid line); QMC (this work, filled circles); PQSCHA (dashed line); high-temperature expansion (dotted line); and experiment (open squares). The QMC data connect the regimes where the various methods apply.

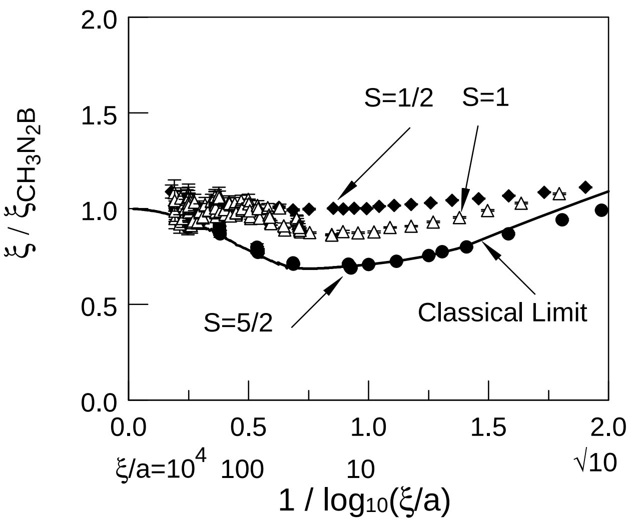

FIG. 3. Ratio of correlation length ξ to CH_3N_2B prediction, vs. ξ, for $S = 1/2, 1, 5/2, \infty$. By $S = 5/2$ the residual deviation essentially reached the classical $S \to \infty$ limit.